Feasibility of nonlinear absorbers for transient vibration reduction

F. Petit, M. Loccufier, D. Aeyels
Ghent University, SYSTeMs Research Group,
Technologiepark Zwijnaarde 914, 9052, Gent, Belgium
e-mail: **frits.petit@ugent.be**

Abstract

Torsional vibrations are a cause of severe damage to flexible couplings and gearboxes of a dredger drive line. In this paper the feasibility of three different vibration absorbers is discussed when reducing transient vibrations originating from sudden load changes. The classical linear absorber is compared to two nonlinear ones, one with a cubic spring (known as the nonlinear energy sink or NES) and one with a combination of a linear and a cubic spring (a Duffing type absorber). Both nonlinear absorbers succeed in achieving a multimodal vibration reduction, whereas the linear absorber can only mitigate a single vibration mode. The most important reduction is however obtained in the initial phase where the energy of one vibration mode is decreased through a beating phenomenon. A much slower energy reduction of the remaining vibration modes takes place after this initial phase. As a result, both the NES and the Duffing type absorber still need to be tuned to the most important mode, despite their ability to mitigate multiple modes.

1 Introduction

As the activities of dredger ships are increasing throughout the world, their durability and maintenance is receiving considerable attention. However, the drive line of a dredger still suffers from early damage at vital components like elastic couplings and gear boxes which connect the dredger's main equipment, namely the propeller, the generator, the diesel engine and the pump. This early damage is primarily caused by excessive torsional vibrations that originate from transient behavior such as engaging and disengaging propeller and pump clutches, altering the vessel's speed and changing the propeller pitch. Here, the specific case of a trailing suction hopper dredger is considered as this type of ship is, more than any other, characterized by highly frequent transient behavior. Indeed, as the configuration and operating conditions of a hopper dredger are changed that often, one could almost regard the transient behavior as an everlasting one. ([1]).

When removing the source of vibration or altering the structure itself is not possible, other means of reducing excessive vibrations have to be considered. A well-established method to mitigate vibrations in machinery is to attach to the structure, a lightweight damped spring-mass element known as the tuned mass damper or vibration absorber, which was originally proposed by Frahm [2] and later optimized for both harmonic ([3]) and transient excitations ([4], [5]). This device is, however, tuned to a single frequency and therefore loses efficiency when more than one vibration mode contributes to the overall response. Because this is the case for the dredger drive line, an adapted version of this classical vibration absorber is required. Logical extensions that do allow multimodal vibration reduction, are the multi-degree-of-freedom vibration absorber ([6]) and multiple vibration absorbers each tuned to a different frequency ([7]). However, as the available attachment space on the dredger drive line is highly limited, these two alternatives lose applicability.

Recently there has been a growing interest in the study of a strongly nonlinear vibration absorber, known

as the nonlinear energy sink (NES). For a detailed description thereof, see [8]. As opposed to the linear vibration absorber, the NES is not tuned to a single frequency due to its strongly nonlinear (nonlinearisable) stiffness. Hence, this compact device is capable of resonating at any frequency enabling a multimodal vibration reduction. A major drawback of the NES is its inherent frequency-energy dependence. For unimodal vibration, this results in the existence of a well-defined threshold of the input energy below which the NES is ineffective. Above this energy threshold, a so called resonance capture initiates a targeted energy transfer (TET) from the main structure to the NES where the energy dissipation takes place. For multimodal vibration, each vibration mode features a different energy threshold. As described by [9], this results in resonance capture cascades where the NES sequentially resonates with different vibration modes.

In this paper, the vibration reduction capability with respect to the dredger drive line of three types of absorbers are compared, namely the classical linear absorber, the NES and a Duffing-type absorber. The Duffing-type absorber consists of a combination of the linear absorber and the NES as it features linear behaviour for low energy levels and strongly nonlinear cubic behaviour for high energy levels. Although the Duffing-type absorber still exhibits energy thresholds and resonance capture cascades like the NES, different dynamics can be distinguished for lower energy levels.

Because the different energy thresholds are of major importance in the tuning procedure of both nonlinear absorbers, it is explained how these thresholds can be adjusted. In a first step, the drive line is excited such that only one mode dominates the total vibration. By nondimensionizing the equations, the energy thresholds and the influence the nonlinear absorber parameters have on it are investigated. The results obtained for this unimodal case, are then further used in the multimodal case where the absorbers are tuned to the most important vibration mode.

Both nonlinear absorbers succeed in achieving a multimodal vibration reduction. The most important reduction is however obtained in the initial phase where the energy of one vibration mode is decreased by a beating phenomenon which is also present in the case of the linear absorber. After this initial phase a much slower energy reduction of the remaining vibration modes takes place. This means that, despite their ability to mitigate multiple modes, both the NES and the Duffing type absorber still need to be tuned to the most important mode. Limiting the frequency interval to the most important modes by using a Duffing type absorber, shows however no improvement compared to the NES where every frequency can theoretically be attained.

Section 2 presents an overview of the hopper dredger drive line, its modelling approach used throughout the paper as well as the most important transient loads. Then, a brief introduction of the NES is presented in Section 3. The influence of the NES parameters on the energy thresholds is discussed in Section 4 and applied to both unimodal and multimodal case in Sections 5 and 6. Finally Section 7 presents the feasibility of using a Duffing type absorber.

2 A trailing suction hopper dredger

A hopper dredger has become an indispensable ship in the maritime world ([10]). It is mainly used to deepen waterways (harbors, rivers) in order to keep them navigable. However, the most well-known purpose is probably land reclamation.

2.1 Layout of a dredger

Figure 1 shows a possible layout of the drive line of a hopper dredger. In most cases a hopper dredger contains two such drive lines working independently of each other, one at the port side and one at the starboard side. The main components (engine, pump, generator and propeller) are connected through gear boxes and flexible couplings. Further more, clutches can be engaged and disengaged to allow a change of the drive line's configuration, i.e. the pump and the propeller can be connected and disconnected.

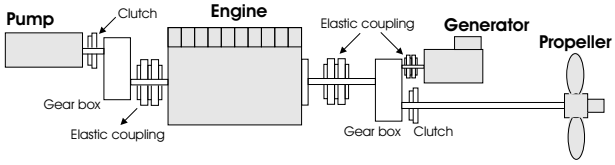

Figure 1: Outline of a hopper dredger

The main tool of a hopper dredger is a centrifugal pump. This pump sucks up mud through a trailing suction pipe and collects it in the hopper. When this hopper is filled, the pump clutch is disengaged and the ship sails towards the place of discharge. Discharging the ship can be done by simply opening the bottom doors of the hopper. Another way is to reengage the pump clutch, thereby pressing the load ashore through pipes, or rainbowing the load close to the ship by means of a nozzle. Finally, the ship sails back unloaded and the cycle recommences. Each step in this cycle requires a change in the configuration of the drive line.

2.2 Sources of vibration

Before commissioning, classification societies demand extensive torsional vibration calculations (TVC-analysis) of the dredger drive line to prevent serious shortcomings. The main sources of vibration taken into account in this analysis, are the irregular driving torque of the diesel engine and the excitation generated by the propeller. While these periodic excitations definitely take priority in a vibration analysis, this paper is limited to the analysis of transient loads (e.g. start-up, engaging and disengaging clutches), as they have shown to be a source of severe damage to couplings and gear boxes. The most important sudden load changes are initiated by engaging and disengaging the propeller and pump clutches, by changing the load on the generator and by altering the speed of the diesel engine. Interestingly, they all occur at different places on the drive line. As a result, different vibration modes are excited, again supporting the usefulness of a nonlinear absorber.

2.3 A reduced model of the hopper dredger drive line

In the obliged TVC-analysis, the continuous drive line shown in Fig. 1 is modelled as a lumped parameter model according to methods explained in [11]. However, in practice this model still contains up to 50 degrees of freedom making it computationally heavy. Further more, from the point of view of a vibration control engineer, it is far too complex. Therefore, a simplified model is developed, still detailed enough to explain the major phenomena.

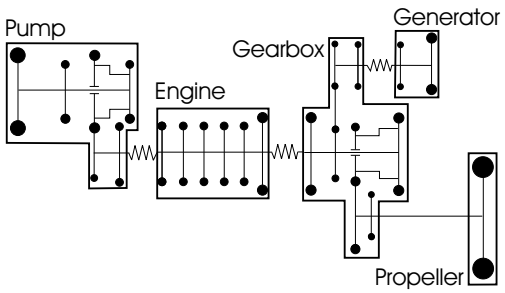

Figure 2: Reduced model of the mass-elastic system

In a first step, every stiffness and inertia is reduced to the engine speed. Secondly, the drive line is only allowed to twist at the flexible couplings, because their stiffness is much lower (factor 10) than that of other shaft elements. An exception to this rule is the propeller shaft, which also features a low stiffness due to its

long length. All remaining inertias are assumed to be rigidly connected, creating different blocks as shown in Fig. 2. As a result, the 50 degrees of freedom of the original model are reduced to 5. The eigenfrequencies ω_i (with $\omega_1 = 0$) and the corresponding mass matrix normalized eigenvectors e_i of the reduced model are presented in Table 1. The percentage error between the eigenfrequencies of the original and the reduced model is shown to be well below the engineering 5%.

Table 1: Modal parameters

	e_1	e_2	e_3	e_4	e_5
Pump	0.0096	-0.0121	0.0086	-0.0041	-0.0001
Diesel	0.0096	-0.0021	-0.0083	0.0115	0.0015
Gear box	0.0096	0.0058	-0.0076	-0.0104	-0.0159
Propeller	0.0096	0.0063	-0.0094	-0.0166	0.0234
Generator	0.0096	0.0162	0.0146	0.0053	0.0013
ω_i (rad/s)	0	10.42	16.06	22.42	47.34
Error (%)	0	3.15	2.84	3.38	3.32

3 The nonlinear energy sink (NES)

This section explains the basic philosophy behind the NES by comparing it with the classical linear vibration absorber. When attaching this linear absorber to an undamped single-degree-of-freedom (SDOF) system, the dynamics are governed by:

$$m\ddot{x} + kx + c_a(\dot{x} - \dot{x}_a) + k_a(x - x_a) = 0 \tag{1}$$

$$m_a\ddot{x}_a + c_a(\dot{x}_a - \dot{x}) + k_a(x_a - x) = 0 \tag{2}$$

where m and k denote the mass and stiffness of the main system, while subscript a is used for the absorber. Damping is assumed to be viscous with damping factor c_a. For an optimal reduction of the vibration amplitude, the natural frequency of the absorber ω_a needs to be tuned to that of the main system:

$$\omega_a = \sqrt{\frac{k_a}{m_a}} \approx \sqrt{\frac{k}{m}} \tag{3}$$

Assuming $m_a << m$, the natural frequencies of the combined system are very close to each other. As a result, the overall response is dominated by the beating phenomenon, as displayed in Fig. 4 ([3]).

Regarding the NES, the same tuning principle (3) holds. However, as this nonlinear oscillator exhibits a frequency-energy dependence, it does not posses a natural frequency. To overcome this problem, an equivalent natural frequency is defined by applying the harmonic balance method on the undamped equation of motion of the NES ([12]):

$$m_{\text{NES}}\ddot{x}_{\text{NES}} + k_{\text{NES}}x_{\text{NES}}^3 = 0 \tag{4}$$

where m_{NES} and k_{NES} denote the NES mass and cubic spring constant. Substituting $x_{\text{NES}}(t) = \frac{A}{\omega}\sin\omega t$ ($\dot{x}_{\text{NES}}(0) = A$, $x_{\text{NES}}(0) = 0$) as a solution in (4), and balancing the fundamental harmonic, yields:

$$A^2 = \frac{4}{3}\frac{m_{\text{NES}}\omega^4}{k_{\text{NES}}} \tag{5}$$

The equivalent natural frequency ω_{eq} becomes:

$$\omega_{eq} = [\frac{3}{4}\frac{k_{\text{NES}}A^2}{m_{\text{NES}}}]^{1/4} \tag{6}$$

and increases with energy (initial velocity A) due to the hardening spring as illustrated in Fig. 3.

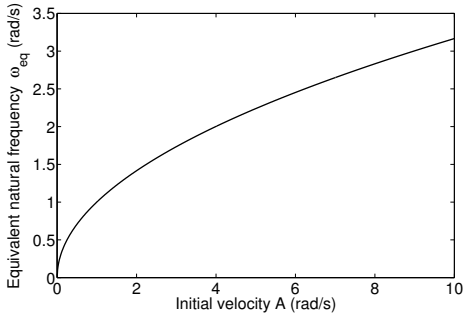

Figure 3: Frequency-energy dependence of the NES

Hence, when the NES is attached to a SDOF structure, it is expected to achieve optimal vibration reduction in a certain energy interval, due to the frequency-tuning principle (3). Although this is indeed the case, more complicated phenomena occur which can not be explained by ω_{eq}. This is illustrated in Fig. 5, where a viscously damped NES (with damping factor c_{NES}) is attached to a SDOF structure, for two different initial conditions. Increasing $\dot{x}(0)$ from 0.5 to 0.6, causes a sudden increase in both the NES response and its efficiency in reducing vibrations. Although Fig. 6 confirms that ω_{eq} indeed reaches the natural frequency of the main system ($\omega = 1$ rad/s) for $\dot{x}(0) = 0.6$, thereby fulfilling (3), some issues still remain.

The sudden increase of NES response, defines an energy threshold, below which no efficient vibration reduction is possible. Such behavior is remarkably different from that of the linear absorber where this energy dependence is not present (Fig. 4).

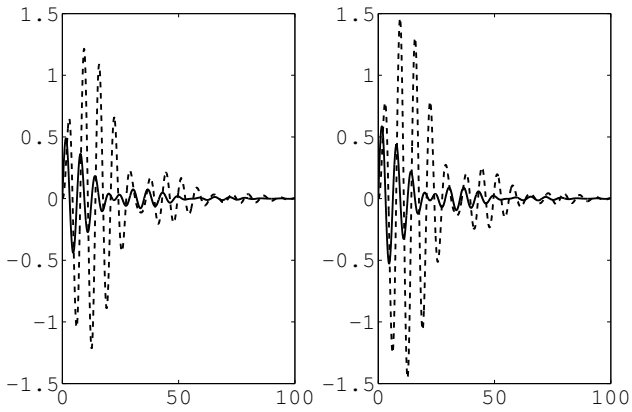

Figure 4: Main system and absorber response ($m = 1, c = 0, k = 1, m_a = 0.05, c_a = 0.01, k_a = 0.045$);
Left: $\dot{x}(0) = 0.5$, $x(0) = \dot{x}_a(0) = x_a(0) = 0$ Right: $\dot{x}(0) = 0.6$, $x(0) = \dot{x}_a(0) = x_a(0) = 0$

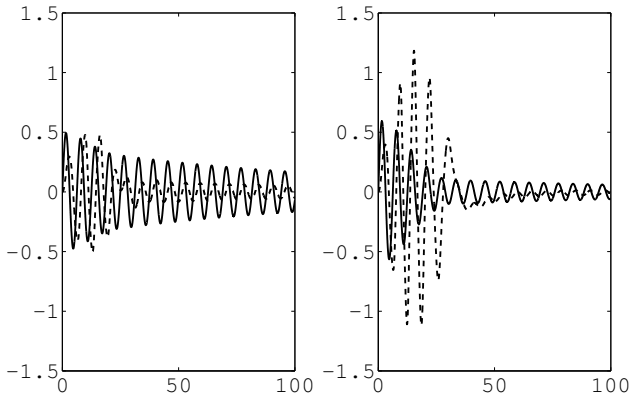

Figure 5: Main system and NES response ($m = 1, c = 0, k = 1, m_{\text{NES}} = 0.05, c_{\text{NES}} = 0.016, k_{\text{NES}} = 0.067$,); Left: $\dot{x}(0) = 0.5, x(0) = \dot{x}_{\text{NES}}(0) = x_{\text{NES}}(0) = 0$ Right: $\dot{x}(0) = 0.6, x(0) = \dot{x}_{\text{NES}}(0) = x_{\text{NES}}(0) = 0$

Above the energy threshold, the NES response exhibits a nonlinear beating phenomenon (Fig. 5), closely resembling that of the linear absorber. However, this nonlinear beating phenomenon is only temporarily as due to energy dissipation, relation (3) no longer holds. This is illustrated in Fig. 6 where the equivalent frequency of the NES reaches the natural frequency of the main system ($\omega = 1$ rad/s) for $t \approx 10s$ and rapidly decreases after $t \approx 30s$. Surprisingly, for $t \geq 30s$, both the main structure and the NES attached to it, still vibrate with the same frequency of 1 rad/s (Fig. 5). Hence, for $t \geq 30s$, the equivalent natural frequency given by (6) fails to predict the actual frequency of the NES. In conclusion, the ω_{eq} is an interesting concept to gain initial understanding in the working principle of the NES. It falls short because ω_{eq} is calculated according to the free response of the NES (4). The next section shows that, at least in the undamped case, the NES is actually harmonically excited, so one has to consider the forced response.

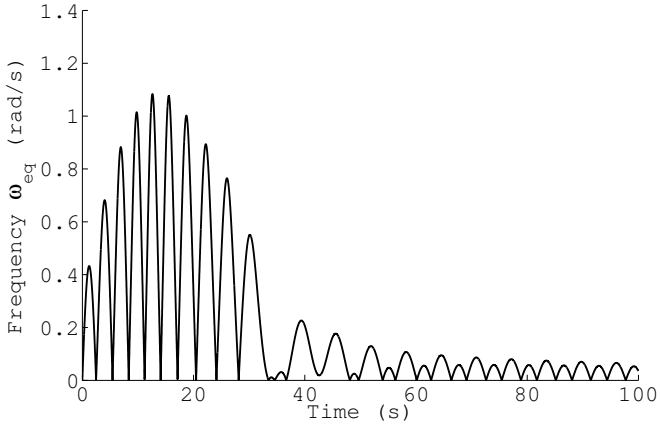

Figure 6: Equivalent frequency as a function of time

4 Parametric study of the energy thresholds: unimodal case

The existence of an energy threshold for SDOF structures, as discussed in the previous section, can be extended to the MDOF case where each vibration mode is characterized by a different energy threshold. In this section, the influence on these energy thresholds of the NES parameters (m_{NES}, c_{NES}, k_{NES}) is investigated for the case of the MDOF dredger drive line of Section 2.3. The analysis is limited to the unimodal case, which means that the initial conditions are chosen according to eigenvectors $e_i, i = 1, ...5$, such that one

vibration mode dominates the response. This allows to consider the MDOF system as 5 SDOF systems which facilitates the analysis. Such a general SDOF system is considered in the next subsection.

4.1 Alternative analysis

To simplify the analysis, both main system (SDOF) and attached NES are considered to be undamped yielding following equations of motion:

$$m\ddot{x} + kx + k_{\text{NES}}(x - x_{\text{NES}})^3 = 0 \tag{7}$$

$$m_{\text{NES}}\ddot{x}_{\text{NES}} + k_{\text{NES}}(x_{\text{NES}} - x)^3 = 0 \tag{8}$$

Because $m_{\text{NES}} << m$, the response of the main system closely follows that of the main system without NES , i.e. $x(t) \approx \frac{\dot{x}(0)}{\omega} \sin \omega t$ with $\omega = \sqrt{\frac{k}{m}}$(although a small difference in frequency ω disturbs the resemblance for large t). Therefore, we replace the main system by a sinusoidally moving ground z as shown in Fig. 7.

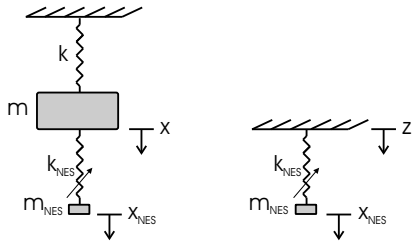

Figure 7: Main system replaced with sinusoidally moving ground z

The equation of motion of this simplified system becomes:

$$m_{\text{NES}}\ddot{x}_{\text{NES}} + k_{\text{NES}}(x_{\text{NES}} - z)^3 = 0 \tag{9}$$

with $z = \frac{\dot{x}(0)}{\omega} \sin \omega t$. Introducing the relative displacement $x_r = x_{\text{NES}} - z$, (9) becomes:

$$m_{\text{NES}}\ddot{x_r} + k_{\text{NES}}(x_r)^3 = m_{\text{NES}}\omega\dot{x}(0) \sin \omega t \tag{10}$$

with initial conditions $x_r(0) = 0, \dot{x}_r(0) = -\dot{x}(0)$. Equation (10) shows that the original two-degree-of-freedom system in free response is approximated by a harmonically excited single-degree-of-freedom system.

4.2 Dimensionless system

Analyzing (10) is not straightforward because it contains 4 different parameters, namely m_{NES}, k_{NES}, ω and $\dot{x}(0)$. Expressing (10) in dimensionless form severely facilitates the analysis as these four parameters can be joined together into only one dimensionless group. First a dimensionless time $\tau = \omega t$ is introduced. In this new time τ, first and second derivatives of x_r become:

$$\dot{x}_r = \frac{dx_r}{dt} = \frac{dx_r}{d\tau}\frac{d\tau}{dt} = \frac{dx_r}{d\tau}\omega \tag{11}$$

$$\ddot{x}_r = \frac{d}{dt}\frac{dx_r}{d\tau}\omega = \frac{d^2x_r}{d\tau^2}\omega^2 \tag{12}$$

changing (10) into:

$$m_{\text{NES}}\omega^2\frac{d^2x_r}{d\tau^2} + k_{\text{NES}}x_r^3 = m_{\text{NES}}\omega\dot{x}(0) \sin \tau \tag{13}$$

with initial conditions $x_r(0) = 0, \dot{x}_r(0) = -\frac{\dot{x}(0)}{\omega}$. Secondly, a dimensionless coordinate x_d is introduced:

$$x_d = \frac{x_r \omega}{\dot{x}(0)} \tag{14}$$

Substituting (14) in (13) yields:

$$m_{\text{NES}}\omega^2 \frac{\dot{x}(0)}{\omega} \frac{d^2 x_d}{d\tau^2} + k_{\text{NES}} \frac{\dot{x}(0)^3}{\omega^3} x_d^3 = m_{\text{NES}}\omega\dot{x}(0)\sin\tau \tag{15}$$

with initial conditions $x_d(0) = 0, \dot{x}_d(0) = -1$. Finally, dividing both sides of (15) by $m_{\text{NES}}\omega\dot{x}(0)$, the dimensionless form of (10) becomes:

$$\frac{d^2 x_d}{d\tau^2} + \gamma x_d^3 = \sin\tau \tag{16}$$

with initial conditions $x_d(0) = 0, \dot{x}_d(0) = -1$. Note that all four parameters $m_{\text{NES}}, k_{\text{NES}}, \omega$, and $\dot{x}(0)$ are joined into one single dimensionless parameter γ:

$$\gamma = \frac{k_{\text{NES}}\dot{x}(0)^2}{m_{\text{NES}}\omega^4} \tag{17}$$

A theoretical analysis of the response x_d as a function of γ is not presented in this article. However, simulations confirm the existence of a threshold for γ above which a sudden rise in the amplitude of x_d appears:

$$\gamma \approx 0.17 \tag{18}$$

This means that the threshold value for $\dot{x}(0)$ is governed by the main system's natural frequency ω and the NES parameters m_{NES} and k_{NES} as follows:

$$\dot{x}(0) \sim \sqrt{\frac{m_{\text{NES}}}{k_{\text{NES}}}}\omega^2 \tag{19}$$

which is exactly the same relation as obtained with the equivalent natural frequency ω_{eq} in (6).

Remarks

- The results obtained can be extended to arbitrary initial conditions where in this case $\tilde{\gamma}$:

$$\tilde{\gamma} = \frac{k_{\text{NES}}}{m_{\text{NES}}} \frac{(\dot{x}(0)^2 + \omega^2 x(0)^2)}{\omega^4} \tag{20}$$

  reaches a threshold value of $\tilde{\gamma} \approx 0.17$.

- The ratio between the thresholds for two different vibration modes i and j is $(\frac{\omega_i}{\omega_j})^2, \omega_i > \omega_j$. This means that this ratio can only be decreased by changing the nonlinear spring characteristic. For example, taking a 5th order spring instead of a cubic spring decreases the ratio to $(\frac{\omega_i}{\omega_j})^{3/2}$. Bringing thresholds closer together could enhance the vibration reduction for multimodal responses discussed in the next section.

4.3 Applied to drive line + errors between real simulation and simplified analysis

An undamped NES is attached to the diesel engine of the dredger drive line with $c_{\text{NES}} = 250$ Nms/rad, $k_{\text{NES}} = 58000$ Nm/rad, and $m_{\text{NES}} = 397/2$ kgm^2, resulting in a moment of inertia relative to the diesel engine of 6%, which is practically feasible.

For every vibration mode i (except mode 1 which is the rigid body mode), the initial velocity vector $|A|e_i$ ($A \in \mathbb{R}$) is increased until a sudden rise in the NES response is visible in the simulation. The corresponding initial velocity (rad/s) at the diesel engine for which this happens, is listed in Table 2 as $\dot{x}_{sim}(0)$. This value is compared with the approximated result derived in the previous section:

$$\dot{x}(0) \approx \sqrt{0.17}\sqrt{\frac{m_{\text{NES}}}{k_{\text{NES}}}}\omega^2 \tag{21}$$

listed as $\dot{x}_{approx}(0)$.

Table 2: Dredger drive line's thresholds

	mode 1	mode 2	mode 3	mode 4	mode 5
$\dot{x}_{sim}(0)$ (rad/s)	-	2.62	6.27	12.16	52.84
$\dot{x}_{approx}(0)$ (rad/s)	-	2.62	6.22	12.12	54.06
Error (%)	-	0	0.8	0.4	2.3

The low error value between $\dot{x}_{sim}(0)$ and $\dot{x}_{approx}(0)$ clearly justifies the use of (21) to estimate the influence of m_{NES}, k_{NES} and ω on the threshold value for $\dot{x}(0)$.

4.4 Influence of c_{NES}

Holding m_{NES} and k_{NES} constant ($m_{\text{NES}} = 397/2$ kgm^2, $k_{\text{NES}} = 58000$ Nm/rad), the influence of c_{NES} on the threshold value for $\dot{x}(0)$ is displayed in Fig. 8 for vibration modes 2, 3, 4 and 5. The threshold values increase only slightly for higher values of c_{NES} over the entire range of c_{NES} (0-1000 Nms/rad) which justifies the analysis of the threshold value performed in the undamped case. For $c_{\text{NES}} > 1000$ Nms/rad, the relative motion between the NES and the diesel engine is almost blocked. Because a sudden increase in the NES response is not possible in this case, energy thresholds can not be defined.

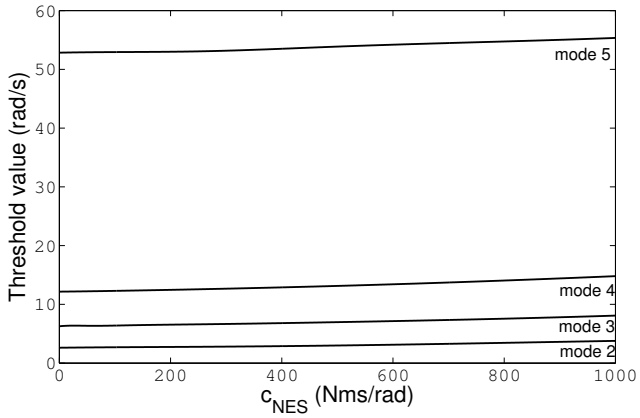

Figure 8: Threshold values for $\dot{x}(0)$ as a function of c_{NES} for different vibration modes

5 Vibration reduction: unimodal case

This section compares the performance of the linear absorber and the NES when the drive line is vibrating according to mode 5 ($\omega_5 = 47.34\ rad/s$), referred to as a unimodal transient vibration response. This is achieved by choosing the initial conditions according to the eigenvector of mode 5. The initial velocity of

the propeller gearbox is chosen $\dot{x}_g(0) = 0.36\ rad/s$. Both absorbers are attached to the propeller gearbox with absorber mass $m_a = m_{\text{NES}} = 397/2\ kgm^2$.

5.1 Linear absorber

The optimal absorber parameters for transient vibration of a SDOF system are given by ([5], pp. 38-46):

$$\frac{\omega_a}{\omega_5} = \frac{1}{1+\mu} \tag{22}$$

$$\zeta_a = \frac{c_a}{2m_a\omega_a} \leq \sqrt{\frac{\mu}{1+\mu}} \tag{23}$$

where μ is the absorber mass relative to the mass of the main system. For MDOF systems, μ can be redefined as the absorber mass relative to the modal mass of mode 5 at the attachment location [13]:

$$\mu = \frac{m_a}{\frac{1}{e_5(3)^2}} = m_a e_5(3)^2 \tag{24}$$

$$= 0.0505 \tag{25}$$

with e_5 the mass-matrix normalized eigenvector corresponding to vibration mode 5. Substituting (25) in (22-23) yields following absorber parameters:

$$m_a = 397/2 kgm^2 \tag{26}$$

$$k_a = 4.03 \cdot 10^5 Nm/rad \tag{27}$$

$$c_a \leq 3.92 \cdot 10^3 Nms/rad \tag{28}$$

For $c_a = 1600\ Nms/rad$, the vibration amplitude of the gearbox is reduced to less than 20% of the value attained without absorber ($7.5 \cdot 10^{-3} rad$). This is achieved after $0.31s$ or less than 3 periods of vibration (Fig. 9).

5.2 NES

According to (17) and (18), the undamped NES reaches its threshold value for:

$$k_{\text{NES}} \geq \frac{0.17 m_{\text{NES}} \omega^4}{(\dot{x}_g(0))^2} = 1.4 \cdot 10^9\ Nm/rad \tag{29}$$

For a damped NES with $c_a = 1600 Nms/rad$, this threshold value increases to $k_{\text{NES}} \geq 2 \cdot 10^9\ Nm/rad$. Here the 20% level is attained after $0.38s$ which is achieved by further increasing k_{NES} to $2.5 \cdot 10^9\ Nm/rad$.

As was expected, the linear absorber performs better than the NES when a single vibration mode is dominating the response. Figure 9 shows a faster vibration reduction with the linear absorber in both short term (3 periods) and long term (10 periods). This can be explained by the fact that the NES frequency is energy dependent causing at a certain instant a mistuning in frequency. On the other hand, the linear absorber is energy independent resulting in a correct tuning frequency at all time.

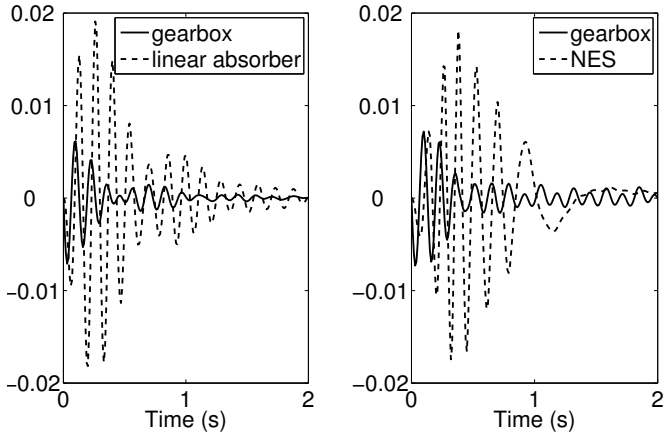

Figure 9: Left: Vibration reduction of mode 5 with linear absorber at the propeller gearbox; Right: Vibration reduction of mode 5 with NES at propeller gearbox

6 Vibration reduction: multimodal case

In practice, the dredger drive line suffers from transient excitations where more than one vibration mode dominates the response. Such a multi-frequency response is clearly illustrated in Fig. (10) for an initial velocity of the propeller of 1 rad/s.

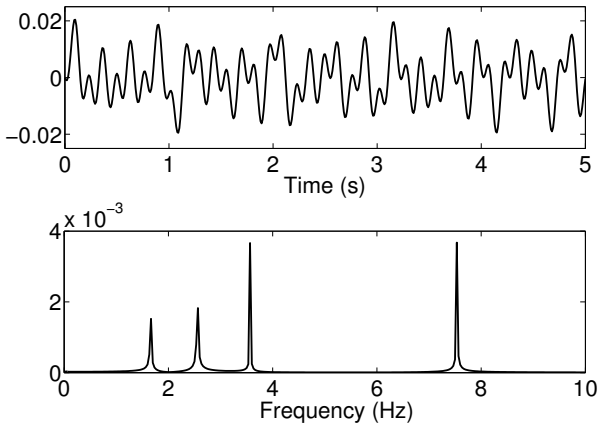

Figure 10: Multimodal response at the propeller gearbox without absorber

The corresponding frequency content shows the presence of two dominant modes (modes $4 = 3.57Hz$ and $5 = 7.53Hz$) while modes 2 ($1.66\ Hz$) and 3 ($2.55\ Hz$) are less important. The vibration reduction capabilities of the linear absorber and the NES are compared when tuned to mode 5. The same absorber parameters can be used as in the unimodal case for both the linear absorber ànd the NES. Indeed, an initial velocity of $1\ rad/s$ at the propeller corresponds to an initial velocity of $0.36\ rad/s$ at the gearbox for mode 5 which was used in the unimodal case to tune the NES.

The response of the gearbox, the time-frequency content (wavelet transform) of the relative motion between gearbox and absorber, and the energy dissipated by the absorber are illustrated in Fig. 11 and 12.

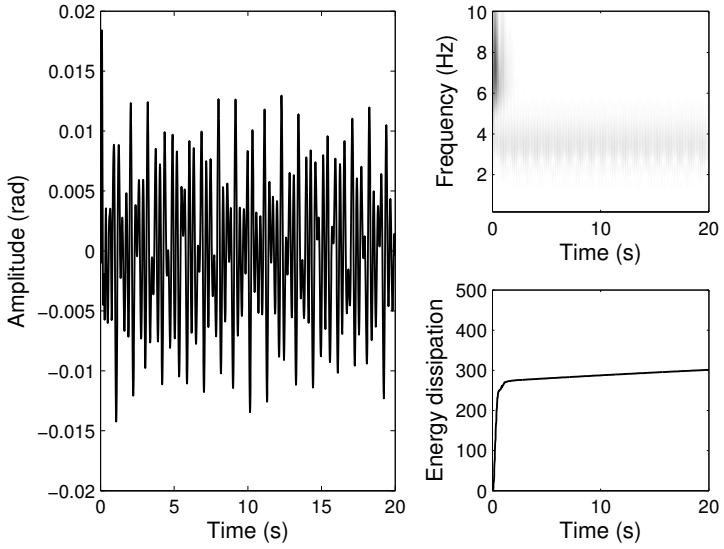

Figure 11: Multimodal response at the gearbox with linear absorber

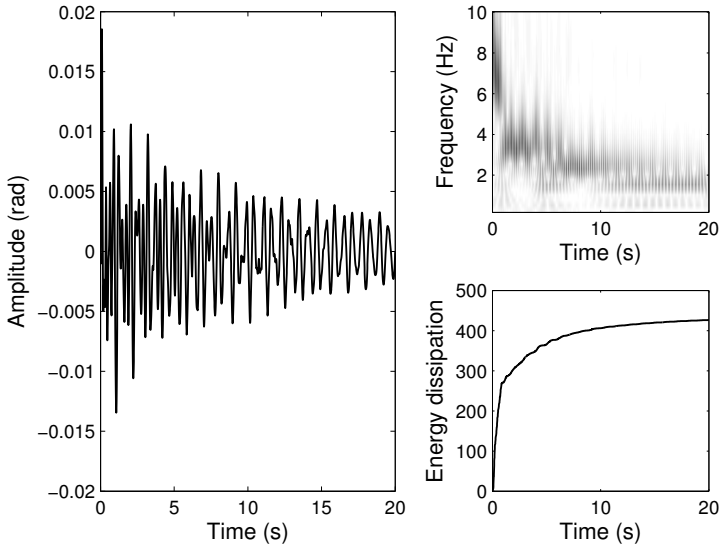

Figure 12: Multimodal response at the gearbox with NES

As evidenced by the wavelet transform, both absorbers initially reduce energy from vibration mode 5 in a similar way. The remaining energy is primarily stored in the other vibration modes which leaves the linear absorber inefficient as it is tuned to mode 5. The NES however succeeds in reducing energy from the other modes as well due to its inherent frequency-energy dependence. These so called resonance capture cascades are clearly visible in the wavelet transform as the frequency changes from that of mode 5 to those of the lower vibration modes. The corresponding decrease of vibration energy is however much slower than that of the initial phase. This means that the NES still needs to be tuned to the most dominant mode, despite its capability to mitigate energy at virtually every frequency.

7 Duffing vibration absorber

The linear absorber focusses on one single frequency while the NES can capture virtually every frequency. As two vibration modes are dominant in the example of Section 6, it is interesting to question whether the vibration reduction can be further improved by focussing on the frequency interval containing these dominant modes. In this section we try to achieve this by using the Duffing vibration absorber with a linear part tuned to the lowest vibration mode 4, while the nonlinear part is designed to reach the threshold for mode 5.

Similar to the NES, an equivalent natural frequency can be defined by considering the free response of the Duffing absorber:

$$m_{\text{DUF}}\ddot{x}_{\text{DUF}} + kx_{\text{DUF}} + a_{\text{DUF}}kx_{\text{DUF}}^3 = 0 \tag{30}$$

Substituting $x_{\text{DUF}}(t) = \frac{A}{\omega}\sin\omega t$ ($\dot{x}_{\text{DUF}}(0) = A$, $x_{\text{DUF}}(0) = 0$) as a solution in (30), and balancing the fundamental harmonic, yields:

$$A^2 = \frac{4\omega^2}{3a_{\text{DUF}}}[\frac{\omega^2}{\omega_4^2} - 1] \tag{31}$$

with $\omega_4^2 = \frac{k}{m_{\text{DUF}}}$. The equivalent natural frequency ω_{eq} initially equals the frequency of vibration mode 4 ($22.4\ rad/s$) and increases with energy (initial velocity A) due to the hardening spring as illustrated in Fig. 13. Compared to the NES, a smaller frequency interval is covered.

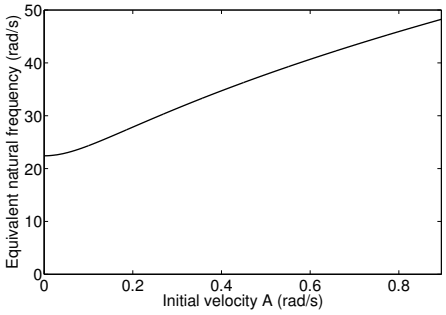

Figure 13: Frequency-energy dependence of the Duffing absorber

The energy threshold for vibration mode 5 can be determined with a dimensionless equation similar to that of the NES:

$$\frac{d^2x_d}{d\tau^2} + \gamma_1 x_d + \gamma_2 x_d^3 = \sin\tau \tag{32}$$

with

$$\gamma_1 = \frac{\omega_4^2}{\omega^2} \tag{33}$$

$$\gamma_2 = a_{\text{DUF}}\omega_4^2\frac{\dot{x}(0)^2}{\omega^4} \tag{34}$$

and initial conditions $x_d(0) = 0, \dot{x}_d(0) = -1$. For $\omega = \omega_5$, $\gamma_1 = 0.22$ and the threshold value for γ_2 becomes $\gamma_2 \geq 0.07$. With an initial velocity at the propeller gearbox $\dot{x}_g(0) = 0.36\ rad/s$, this means the threshold value for a_{DUF} is $a_{\text{DUF}} \geq 5.5 \cdot 10^3$. In the unimodal case with $c_{\text{DUF}} = 1600\ Nms/rad$, a is further increased to $1.8 \cdot 10^4$ to attain a vibration amplitude less than 20% of the initial amplitude after $0.32s$ (Fig. 14).

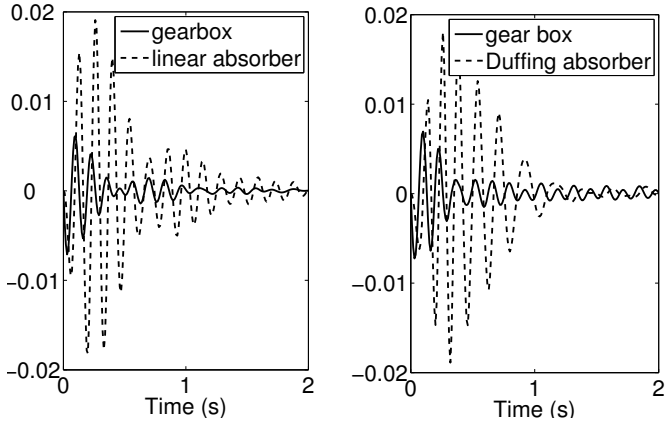

Figure 14: Left: Vibration reduction of mode 5 with linear absorber at the propeller gearbox; Right: Vibration reduction of mode 5 with Duffing absorber at propeller gearbox

Using the same absorber parameters the multimodal vibration reduction is shown in Figure 15.

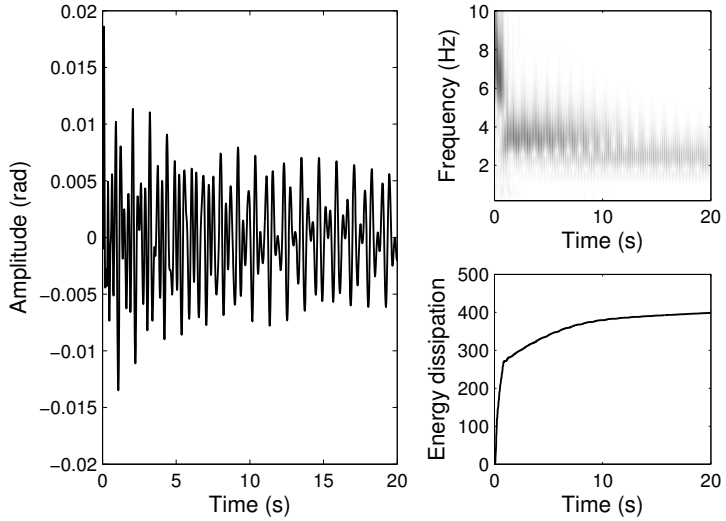

Figure 15: Multimodal response at the gearbox with Duffing absorber

According to the wavelet transform and the corresponding energy dissipation both vibration modes 4 and 5 are reduced. Again, there is a fast reduction in the initial phase as was the case for the linear absorber and the NES. However, focussing on the dominant modes 4 and 5 does not improve the vibration reduction compared to that of the NES.

8 Conclusion

This paper discussed the feasibility of three types of vibration absorbers to suppress transient vibrations on a dredger drive line. The classical linear vibration absorber was compared with two nonlinear ones, namely the NES and a Duffing type absorber. While the linear absorber is capable of reducing only one vibration mode, both nonlinear ones succeed in mitigating multiple modes. Similar to the linear absorber, there is a fast reduction in the initial phase where the energy of one vibration mode rapidly decreases due to a beating phenomenon. After this initial phase, the energy of the remaining vibration modes is reduced in a sequential

manner through so called resonance capture cascades which unfortunately exhibit a much slower vibration reduction. This means that the NES and the Duffing type absorber still need to be tuned to the most prominent mode, despite their ability to tackle virtually every frequency. Moreover, finding a suitable location

References

[1] F. Petit, M. Loccufier, *Torsional Vibrations on a Hopper Dredger due to Transient Conditions*, in *Proceedings of the ASME 2009 IDETC/CIE, San Diego, USA, 2009 August 30-September 2*, San Diego (2009).

[2] H. Frahm, *Device for Damping Vibrations of Bodies*, U.S. patent 989,958 (1911).

[3] J.P. Den Hartog, *Mechanical Vibrations*, McGraw-Hill, New York (1956).

[4] Y.Z. Wang, S.H. Cheng, *The optimal design of dynamic absorber in the time domain and the frequency domain*, Applied Acoustics, Vol. 28, No. 1 (1989), pp. 67-78.

[5] B.G. Korenev, L.M. Reznikov, *Dynamic Vibration Absorbers, Theory and Technical Applications*, Wiley, New York (1993).

[6] L. Zuo, S.A. Nayfeh, *Minimax Optimization of Multi-degree-of-freedom Tuned-mass Dampers*, Journal of Sound and Vibration, Vol. 272, (2004), pp. 893-908.

[7] D.A. Rade, V. Jr Steffen, *Optimisation of Dynamic Vibration Absorbers over a Frequency Band*, Mechanical Systems and Signal Processing, Vol. 14, No. 5 (2000), pp. 679-690.

[8] A.F. Vakakis, O. Gendelman, L.A. Bergman, D.M. McFarland, G. Kerschen, Y.S. Lee, *Nonlinear Targeted Energy Transfer in Mechanical and Structural Systems*, Springer (2009).

[9] G. Kerschen, J. Kowtko, D.M. McFarland, L.A. Bergman, A.F. Vakakis, *Theoretical and Experimental Study of Multimodal Targeted Energy Transfer in a System of Coupled Oscillators*, Nonlinear Dynamics, Vol. 47, No. 1-3 (2007), pp. 285-309.

[10] R.N. Bray, A.D. Bates, *Dredging: A Handbook for Engineers*, John Wiley and Sons Inc., New York (1996).

[11] L.M. Adams, *Rotating Machinery Vibration, From Analysis to Trouble Shooting*, Marcel Dekker Inc., New York (2001).

[12] A.H. Nayfeh, D.T. Mook, *Nonlinear oscillations*, John Wiley & Sons, New York (1995).

[13] R. Rana, T.T. Soong, *Parametric study and simplified design of tuned mass dampers*, Engineering Structures, Vol. 20, No. 3 (1998), pp. 193-204.